

Electronic Supplementary Information for

Multivalent dithiafulvenyl-functionalization of dendritic oligo(phenylene vinylene)s with an anthraquinodimethane core

*Mohammadreza Khadem and Yuming Zhao**

Department of Chemistry, Memorial University of Newfoundland

St. John's, NL, Canada A1B 3X7

Email: yuming@mun.ca

Table of Content

1. Experimental	2
2. NMR Spectra for New Compounds	7
3. UV-Vis Titration Studies	17
4. Molecular Modeling Studies	21
5. SEM Imaging of Poly-[5]	23

1. Experimental

1.1 General

Chemicals were purchased from commercial suppliers and used directly without purification. All reactions were conducted in standard, dry glassware and under an inert atmosphere of nitrogen or argon unless otherwise noted. Evaporation and concentration were carried out with a rotary evaporator. Flash column chromatography was performed with 240-400 mesh silica gel, and thin-layer chromatography (TLC) was carried out with silica gel F254 covered on plastic sheets and visualized by UV light. Melting points (m.p.) were measured using an SRS OptiMelt melting point apparatus and are uncorrected. ^1H and ^{13}C NMR spectra were measured on a Bruker Avance III 300 MHz multinuclear spectrometer. Chemical shifts (δ) are reported in ppm downfield relative to the signals of the internal reference SiMe_4 or residual solvents (CHCl_3 : $\delta_{\text{H}} = 7.24$ ppm, $\delta_{\text{C}} = 77.2$ ppm; CH_2Cl_2 : $\delta_{\text{H}} = 5.32$ ppm, $\delta_{\text{C}} = 54.0$ ppm). Coupling constants (J) are given in Hz. Infrared spectra (IR) were recorded on a Bruker Alfa spectrometer. MALDI-TOF MS analysis was performed on an Applied Biosystems Voyager instrument using dithranol as the matrix. High resolution APPI-TOF MS analysis was done on a GCT premier Micromass Technologies instrument. UV-Vis absorption spectra were measured on a Cary 6000i spectrophotometer. Cyclic voltammetric (CV) and differential pulse voltammetric (DPV) analyses were carried out in a standard three-electrode setup controlled by a BASi Epsilon potentiostat.

Molecular modeling studies were carried out using the Gaussian 09 software.¹ Visualization of the calculated molecular structures and orbitals were done by GaussView 5.²

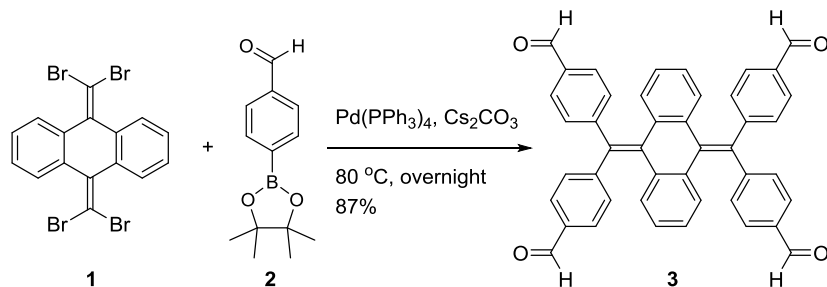
¹ Gaussian 09, Revision E.01, M. J. Frisch, G. W. Trucks, H. B. Schlegel, G. E. Scuseria, M. A. Robb, J. R. Cheeseman, G. Scalmani, V. Barone, B. Mennucci, G. A. Petersson, H. Nakatsuji, M. Caricato, X. Li, H. P. Hratchian, A. F. Izmaylov, J. Bloino, G. Zheng, J. L. Sonnenberg, M. Hada, M. Ehara, K. Toyota, R. Fukuda, J. Hasegawa, M. Ishida, T. Nakajima, Y. Honda, O. Kitao, H. Nakai, T. Vreven, J. A. Montgomery, Jr., J. E. Peralta, F. Ogliaro, M. Bearpark, J. J. Heyd, E. Brothers, K. N. Kudin, V. N. Staroverov, R. Kobayashi, J. Normand, K. Raghavachari, A. Rendell, J. C. Burant, S. S. Iyengar, J. Tomasi, M. Cossi, N. Rega, J. M. Millam, M. Klene, J. E. Knox, J. B. Cross, V. Bakken, C. Adamo, J. Jaramillo, R. Gomperts, R. E. Stratmann, O. Yazyev, A. J. Austin, R. Cammi, C. Pomelli, J. W. Ochterski, R. L. Martin, K. Morokuma, V. G. Zakrzewski, G. A. Voth, P. Salvador, J. J. Dannenberg, S. Dapprich, A. D. Daniels, Ö. Farkas, J. B. Foresman, J. V. Ortiz, J. Cioslowski, and D. J. Fox, *Gaussian, Inc.*, Wallingford CT, 2009.

² GaussView, Version 5, R. Dennington, T. Keith, and J. Millam, *Semichem Inc.*, Shawnee Mission, KS, 2009.

1.2 Synthesis

Compound **2** was purchased from *Combi-Blocks, Inc.* (San Diego, USA). Compounds **1**,³ and **4**⁴ were prepared according to the literature procedures.

Tetraaldehyde-AQ **3**

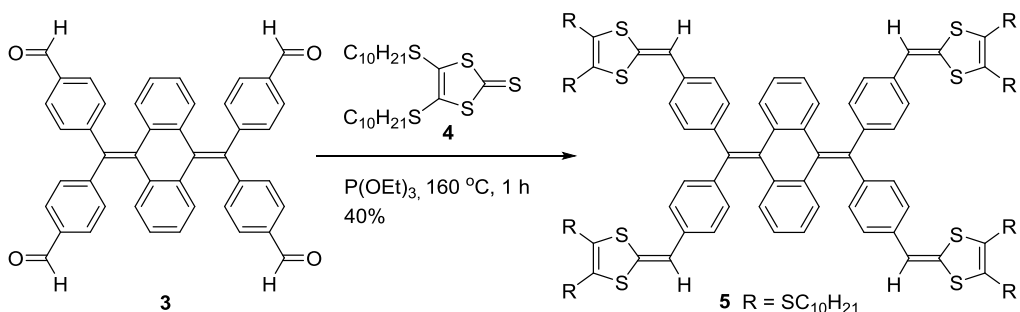


To a 100 mL round-bottomed flask were added 9,10-bis(dibromomethylene)-9,10-dihydroanthracene (**1**) (1.00 g, 1.92 mmol), boronate ester **2** (2.68 g, 11.6 mmol), cesium carbonate (10.0 g, 30.7 mmol), Pd(PPh₃)₄ (0.22 g, 0.19 mmol), THF (50 mL), and deionized water (20 mL). The reaction mixture was stirred and heated at reflux overnight. After that the mixture was cooled down to rt and then poured into brine and extracted twice with CH₂Cl₂. The organic layers were combined and dried over MgSO₄. After filtration and concentration under reduced pressure, the resulting residue was subjected to silica gel column chromatography (hexanes/EtOAc, 4:6) to give compound **3** (1.04 g, 1.67 mmol, 87%) as a pale yellow solid. m.p. 268.2–269.8 °C; IR (neat): 3061, 2923, 2835, 2734, 1699, 1600, 1564 cm⁻¹; ¹H NMR (300 MHz, CD₂Cl₂): δ 10.00 (s, 4H), 7.88 (d, *J* = 8.4 Hz, 8H), 7.64 (d, *J* = 8.1 Hz, 8H), 7.06–7.00 (m, 4H), 6.82–6.76 (m, 4H) ppm; ¹³C NMR (75 MHz, CD₂Cl₂): δ 192.0, 148.1, 138.8, 137.4, 137.3, 135.8, 131.0, 130.4, 128.6, 126.6 ppm; HRMS (APPI-TOF, positive mode) *m/z* calcd for C₄₄H₂₉O₄ 621.2066, found 621.2011 [M + H]⁺. X-ray.

³ (a) Z.-Q. Chen, T. Chen, J.-X. Liu, G.-F. Zhang, C. Li, W.-L. Gong, Z.-J. Xiong, N.-H. Xie, B. Z. Tang and M.-Q. Zhu, *Macromolecules*, 2015, **48**, 7823-7835; (b) S. Pola, C. Kuo, W. Peng, M. M. Islam, I. Chao and Y. Tao, *Chem. Mater.*, 2012, **24**, 2566–2571.

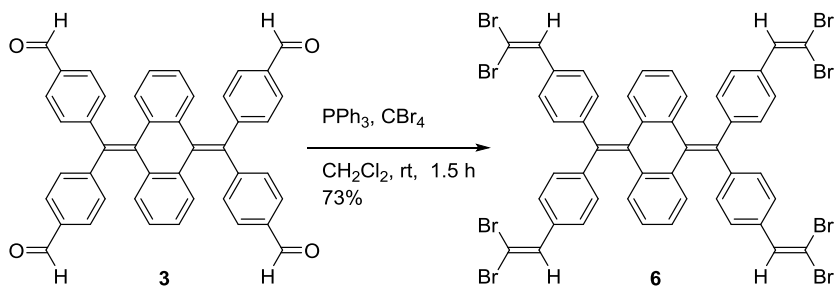
⁴ A. J. Moore and M. R. Bryce, *Tetrahedron Lett.*, 1992, **33**, 1373-1376.

Tetrakis(DTF)-AQ 5



Tetraaldehyde **3** (0.10 g, 0.16 mmol), 1,3-dithiole-2-thione **4** (0.46 g, 0.96 mmol), and $\text{P}(\text{OEt})_3$ (15 mL) were added to a 100 mL round-bottomed flask. The reaction mixture was stirred and heated to 160 °C and kept at this temperature for 1 h. After cooling down to rt, the unreacted $\text{P}(\text{OEt})_3$ was removed by vacuum distillation, and the residue was subjected to silica gel column chromatography (hexanes/ CH_2Cl_2 , 4:1) to give compound **5** (0.15 g, 0.06 mmol, 40%) as a yellow oil. IR (neat): 2953, 2922, 2851, 1570, 1542, 1504, 1464 cm^{-1} ; ^1H NMR (300 MHz, CDCl_3): δ 7.36 (d, $J = 8.3$ Hz, 8H), 7.15 (d, $J = 8.3$ Hz, 8H), 7.05–7.02 (m, 4H), 6.75–6.72 (m, 4H), 6.43 (s, 4H), 2.85–2.80 (m, 16H), 1.67–1.59 (m, 16H), 1.67–1.35 (m, 16H), 1.34–1.19 (m, 112H), 0.92–0.84 (m, 24H) ppm; ^{13}C NMR (75 MHz, CDCl_3) δ 139.7, 139.1, 137.8, 135.8, 134.8, 132.4, 130.2, 128.1, 127.7, 126.7, 125.4, 124.9, 114.0, 36.3, 36.1, 32.0, 29.9, 29.8, 29.7, 29.4, 29.3, 29.2, 28.72, 28.70, 22.8, 14.2 ppm. HRMS (APPI-TOF, positive mode) m/z calcd for $\text{C}_{136}\text{H}_{196}\text{S}_{16}$ 2342.0947, found 2342.0853 $[\text{M} + \text{H}]^+$.

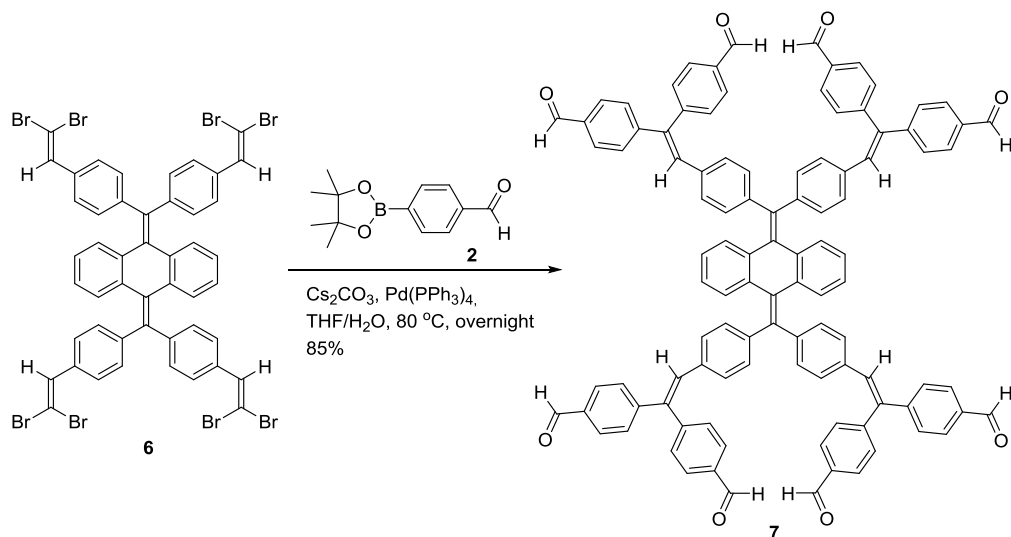
Compound 6



A mixture of CBr_4 (1.55 g, 4.67 mmol) and PPh_3 (1.93 g, 0. mmol) in dry CH_2Cl_2 (100 mL) was stirred at rt. To this solution tetraaldehyde **3** (0.29 g, 0.46 mmol) was slowly added in one portion, and the reaction mixture was kept under stirring at rt for 1.5 h. After that the reaction

mixture was subjected to vacuum filtration and the solids collected were washed with CH_2Cl_2 . The CH_2Cl_2 layers were combined and evaporated to give the crude product of **6**, which was purified by silica gel column chromatography (CH_2Cl_2 /hexanes, 1:4) to give **6** as a white solid (0.42 g, 0.34 mmol, 73%). m.p. > 274 °C (decomp.); IR (neat): 2955, 2923, 2854, 1504, 1459, 880, 865, 843, 760 cm^{-1} ; ^1H NMR (300 MHz, CD_2Cl_2): δ 7.53 (d, $J = 8.1$ Hz, 8H), 7.48 (s, 4H), 7.41 (d, $J = 8.4$ Hz, 8H), 7.03–7.00 (m, 4H), 6.78–6.75 (m, 4H) ppm; ^{13}C NMR (75 MHz, CD_2Cl_2): δ 142.9, 139.4, 137.8, 137.0, 136.4, 134.4, 130.2, 128.9, 128.5, 126.0, 89.9 ppm. HRMS (APPI-TOF, positive mode) m/z calcd for $\text{C}_{48}\text{H}_{29}\text{Br}_8$ 1244.5654, found 1244.5630 [$\text{M} + \text{H}$] $^+$.

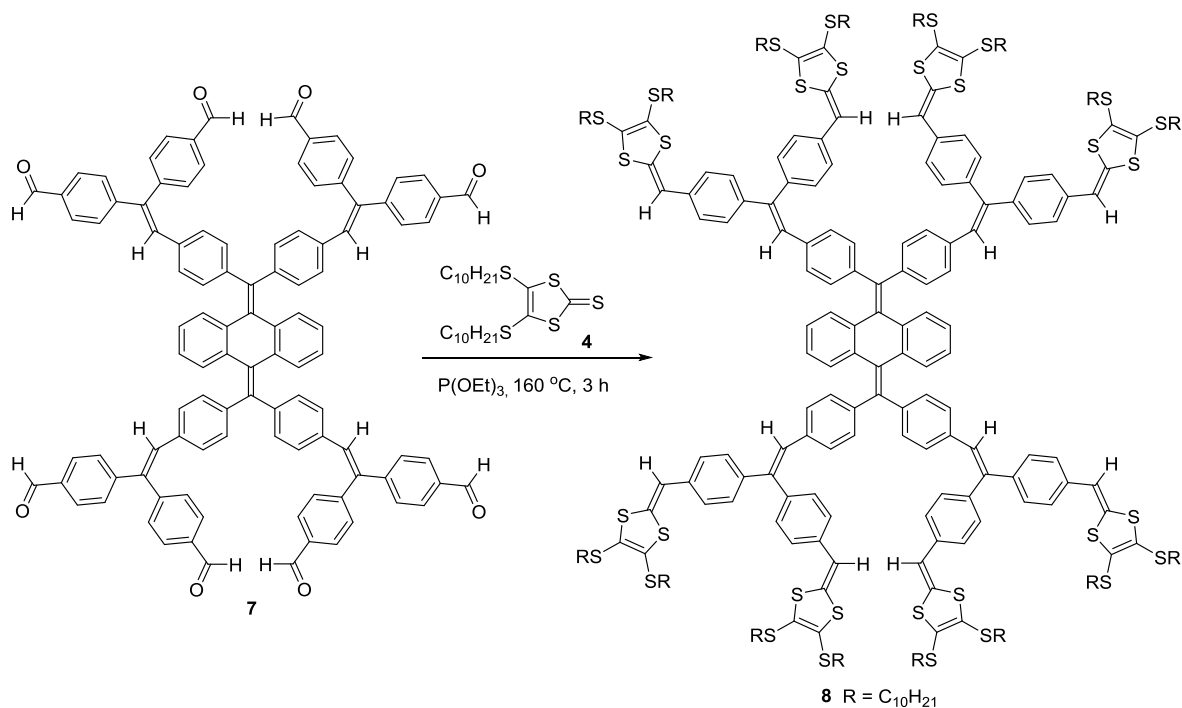
Compound 7



To a 100 mL round-bottomed flask were added compound **6** (0.10 g, 0.080 mmol), boronic ester **2** (0.22 g, 0.96 mmol), cesium carbonate (0.18 g, 0.56 mmol), $\text{Pd}(\text{PPh}_3)_4$ (0.03 g, 0.02 mmol), THF (20 mL), and deionized water (10 mL). The mixture was heated at reflux overnight. After that the mixture was cooled down to rt, poured into brine, and then extracted twice with CH_2Cl_2 . The organic layers were combined and dried over MgSO_4 . After filtration and concentration under reduced pressure, the resulting residue was subjected to silica gel column chromatography (hexanes/EtOAc, 2:3) to give compound **7** (0.98 g, 0.67 mmol, 85%) as yellow oil; IR (neat): 3026, 2827, 2733, 1697, 1595, 1562 cm^{-1} ; ^1H NMR (300 MHz, CD_2Cl_2): δ 10.02 (s, 4H), 10.01 (s, 4H), 7.88–7.83 (m, 16H), 7.49 (d, $J = 8.3$ Hz, 8H), 7.39 (d, $J = 8.1$ Hz, 8H), 7.18 (s, 4H), 7.09 (d, $J = 8.3$ Hz, 8H), 6.93–6.88 (m, 12H), 6.82–6.79 (m, 4 H) ppm; ^{13}C NMR

(75 MHz, CD₂Cl₂): δ 192.1, 192.0, 148.7, 146.7, 142.0, 141.1, 139.4, 137.9, 136.3, 136.2, 135.6, 131.8, 131.7, 130.6, 130.2, 129.9, 128.6, 128.4, 125.8 ppm. HRMS (MALDI-TOF, positive mode) *m/z* calcd for C₁₀₄H₆₈O₈ 1444.4908, found 1444.4907 [M]⁺.

Octa(DTF)-AQ **8**



Octaaldehyde **7** (0.050 g, 0.034 mmol), 1,3-dithiole-2-thione **4** (0.20 g, 0.42 mmol), and P(OEt)₃ (10 mL) were added to a 100 mL round-bottomed flask. The mixture was heated to 160 °C and kept stirring at this temperature for 3 h. After cooling the unreacted P(OEt)₃ was removed by vacuum distillation, and the residue was subjected to silica gel column chromatography (hexanes/CH₂Cl₂, 4:1) to give compound **8** (0.045 g, 0.0092 mmol, 27%) as a yellow oil. IR (neat): 2953, 2923, 2852, 1571, 1544, 1504, 1464 cm⁻¹; ¹H NMR (300 MHz, CD₂Cl₂): δ 7.34–7.31 (m, 8H), 7.21–7.16 (m, 24H), 7.10–7.07 (m, 8H), 6.97–6.92 (m, 16H), 6.82–6.79 (m, 4H), 6.49 (s, 4H), 6.48 (s, 4H), 2.86–2.73 (m, 32H), 1.71–1.52 (m, 32H), 1.48–1.20 (m, 224H), 0.82–0.83 (m, 48H) ppm; ¹³C NMR (75 MHz, CD₂Cl₂): δ 142.4, 141.2, 141.1, 139.9, 138.3, 138.1, 136.6, 136.18, 136.14, 136.0, 133.3, 133.2, 131.3, 129.9, 128.3, 128.1, 127.5, 127.1, 125.4, 125.2, 114.3, 36.68, 36.60, 32.5, 30.6, 30.4, 30.3, 30.2, 30.17, 30.14, 29.95, 29.93, 29.7, 29.17, 29.14, 29.10, 29.0, 23.3 ppm. HRMS (MALDI-TOF, positive mode) *m/z* calcd for C₂₈₈H₄₀₅S₃₂ 4887.2754, found 4887.2319 [M + H]⁺.

2. NMR Spectra for New Compounds

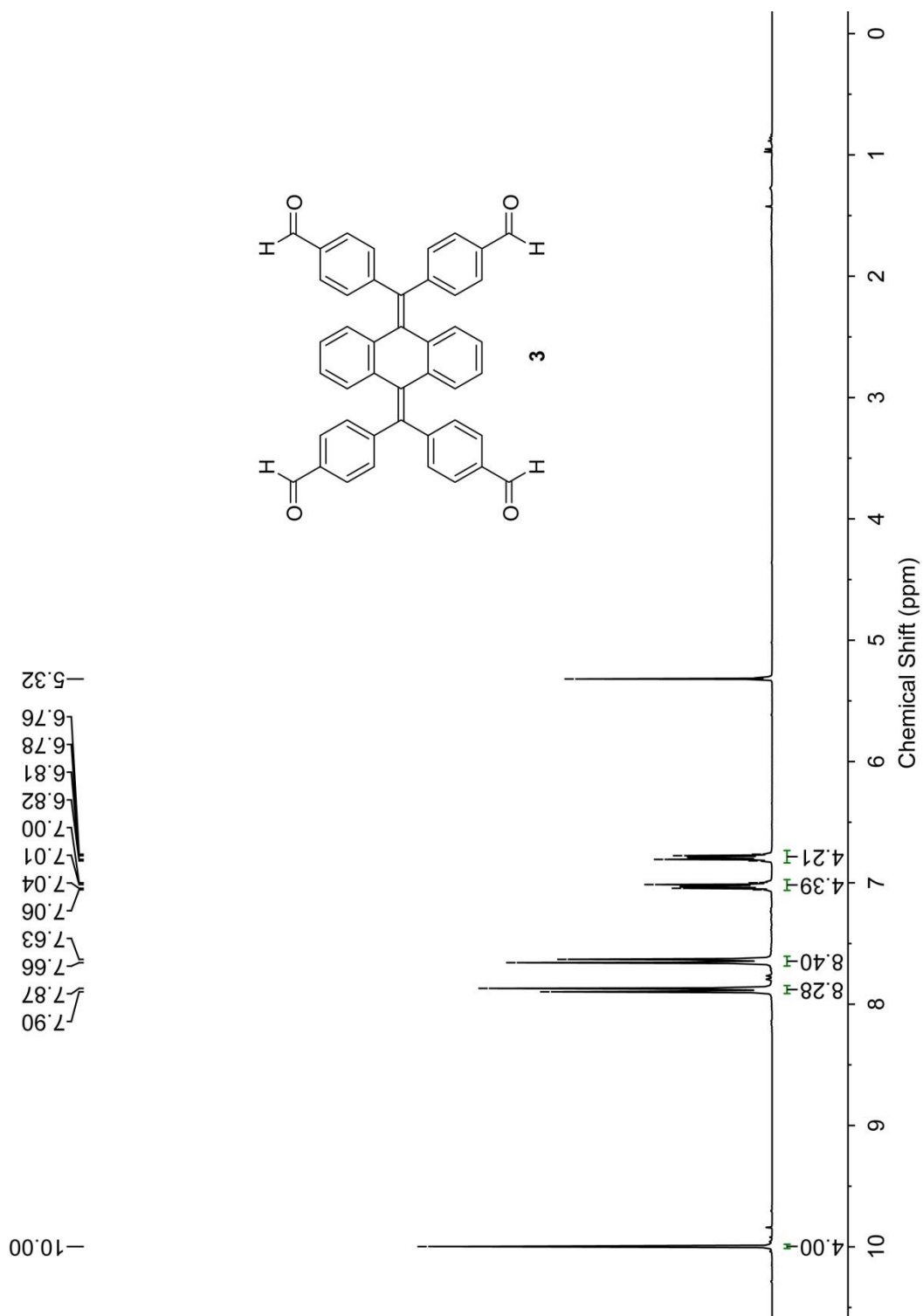


Fig. S-1 ^1H NMR (300 MHz, CD_2Cl_2) of compound 3.

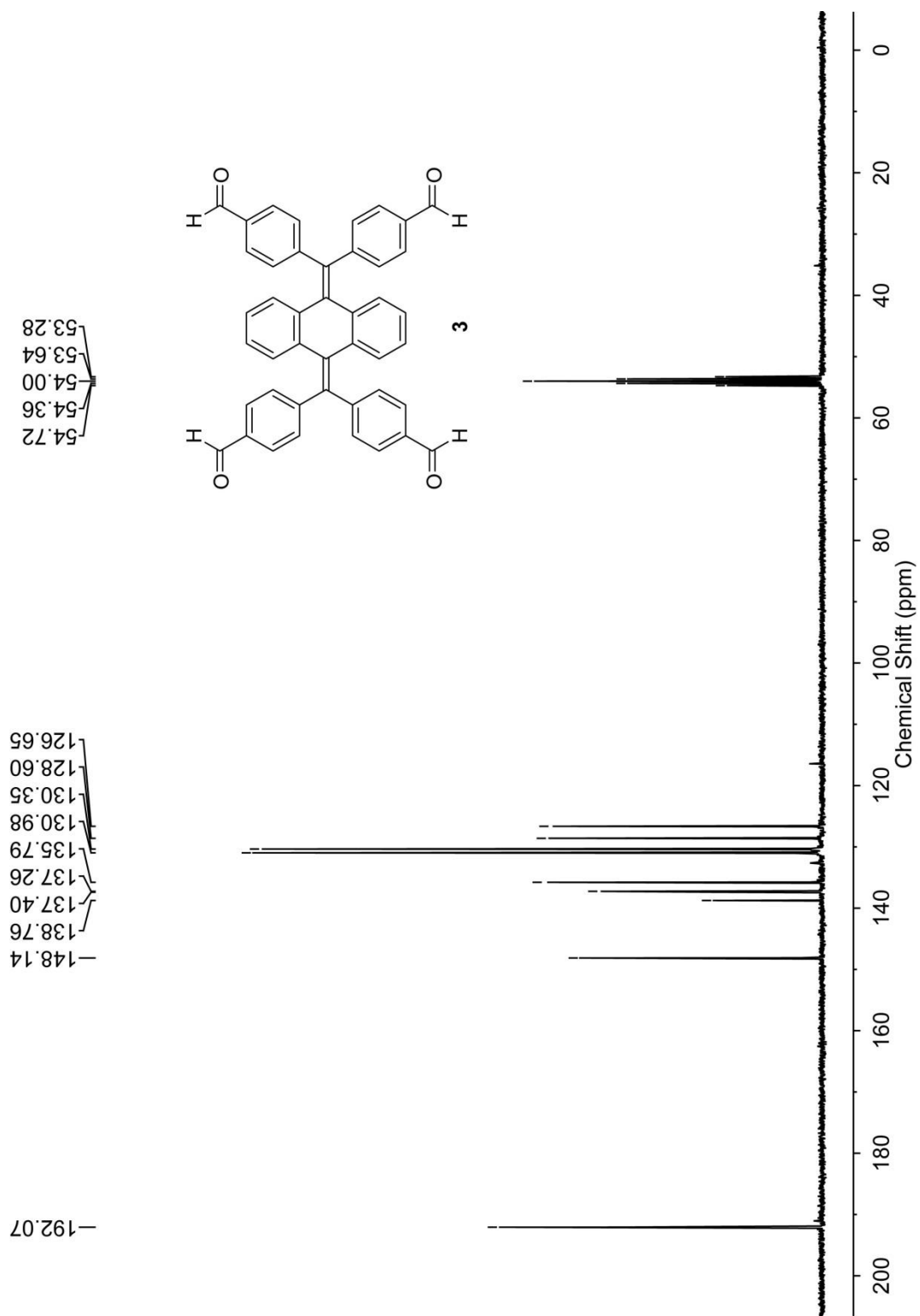


Fig. S-2 ¹³C NMR (75 MHz, CD₂Cl₂) of compound 3.

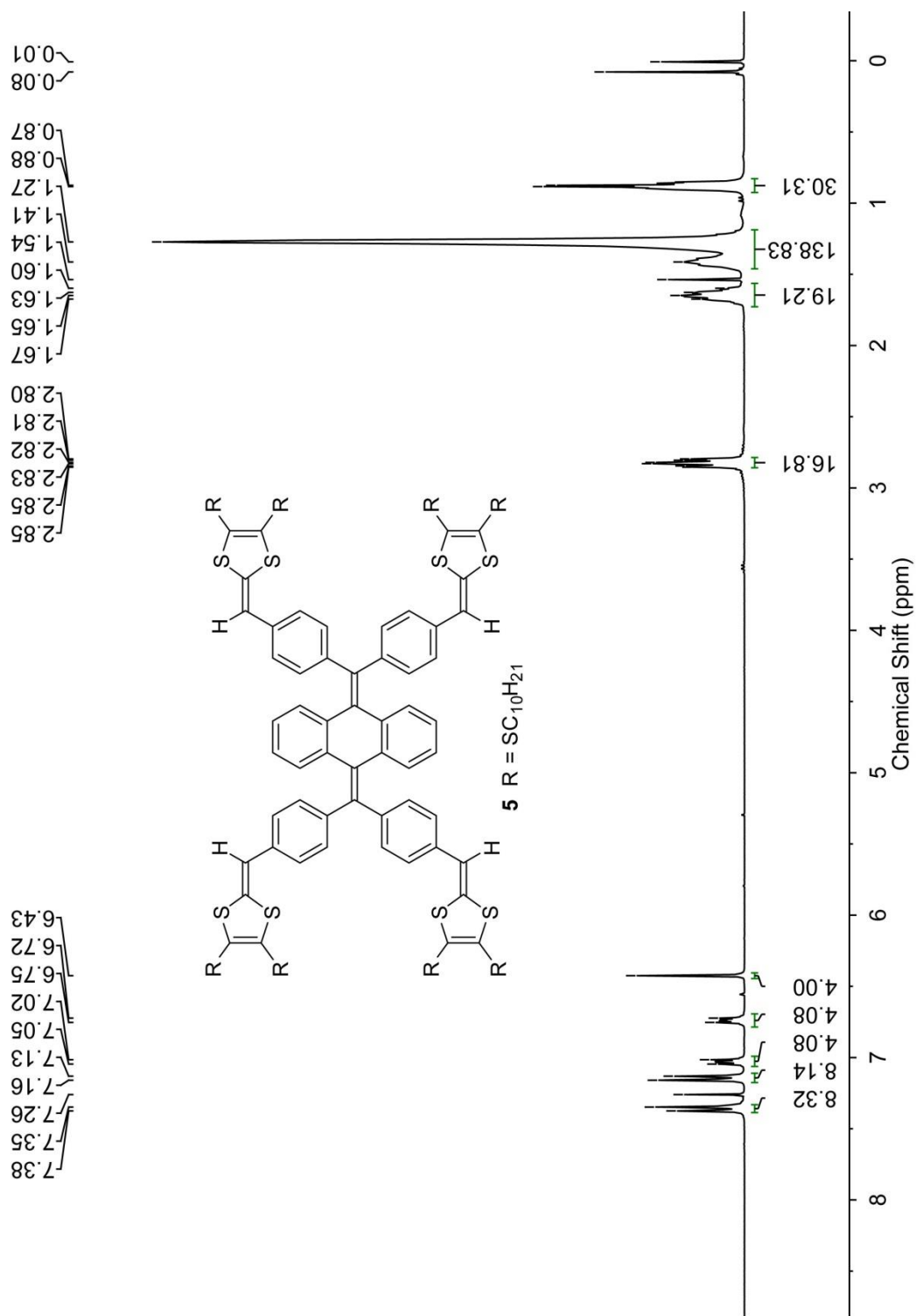


Fig. S-3 ^1H NMR (300 MHz, CDCl₃) of compound 5.

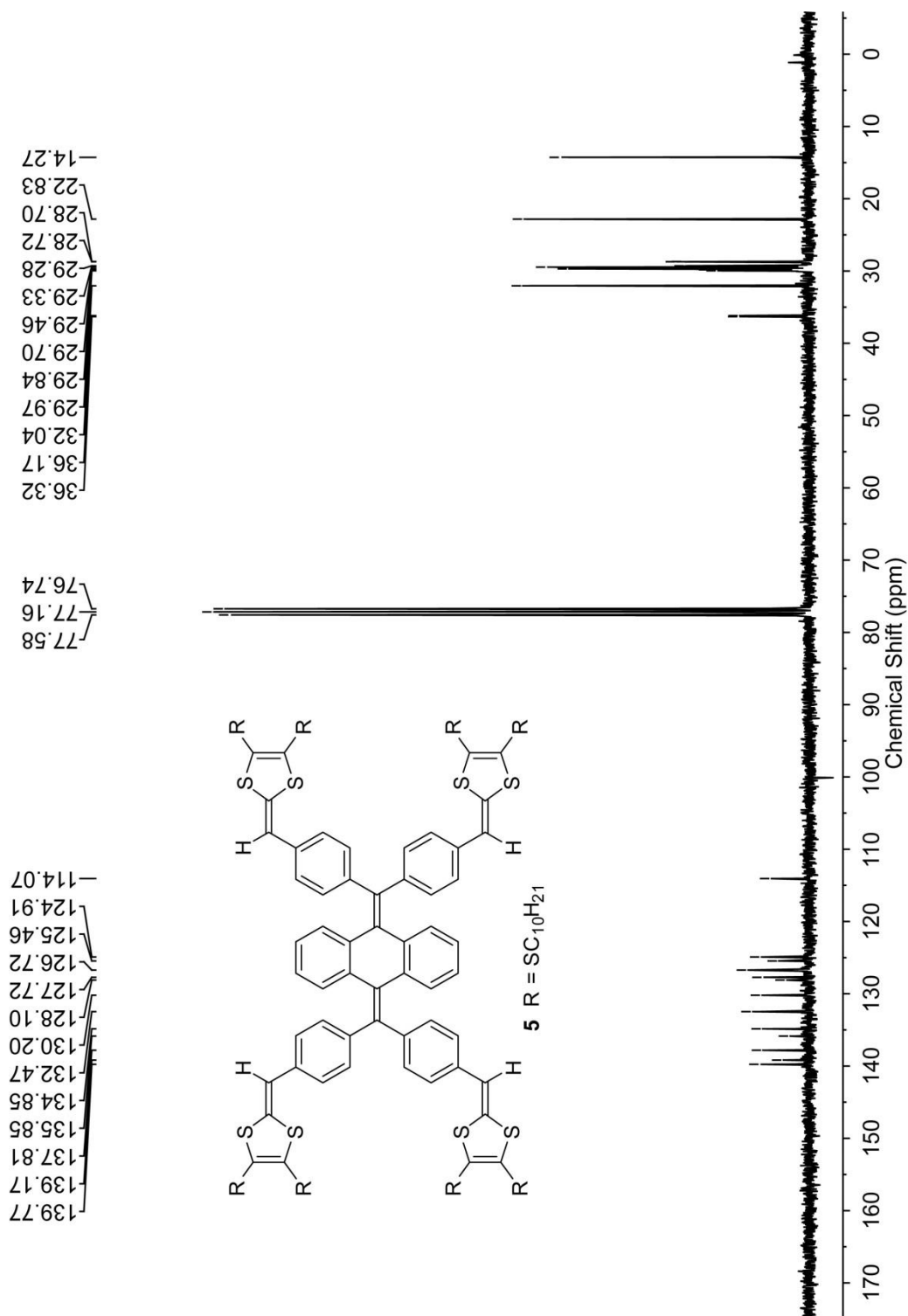


Fig. S-4 ¹³C NMR (75 MHz, CDCl₃) of compound **5**.

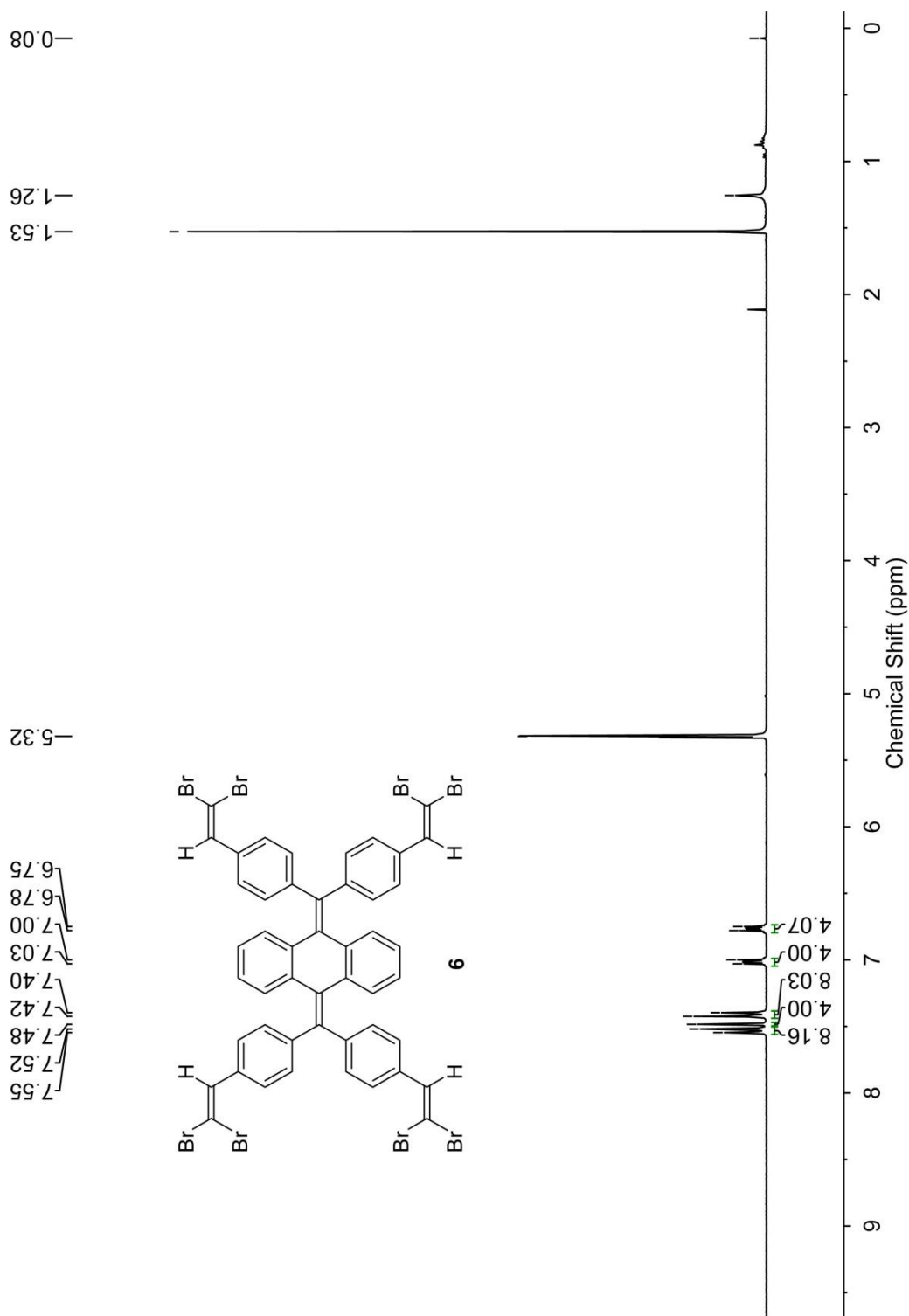


Fig. S-5 ^1H NMR (300 MHz, CD_2Cl_2) of compound **6**.

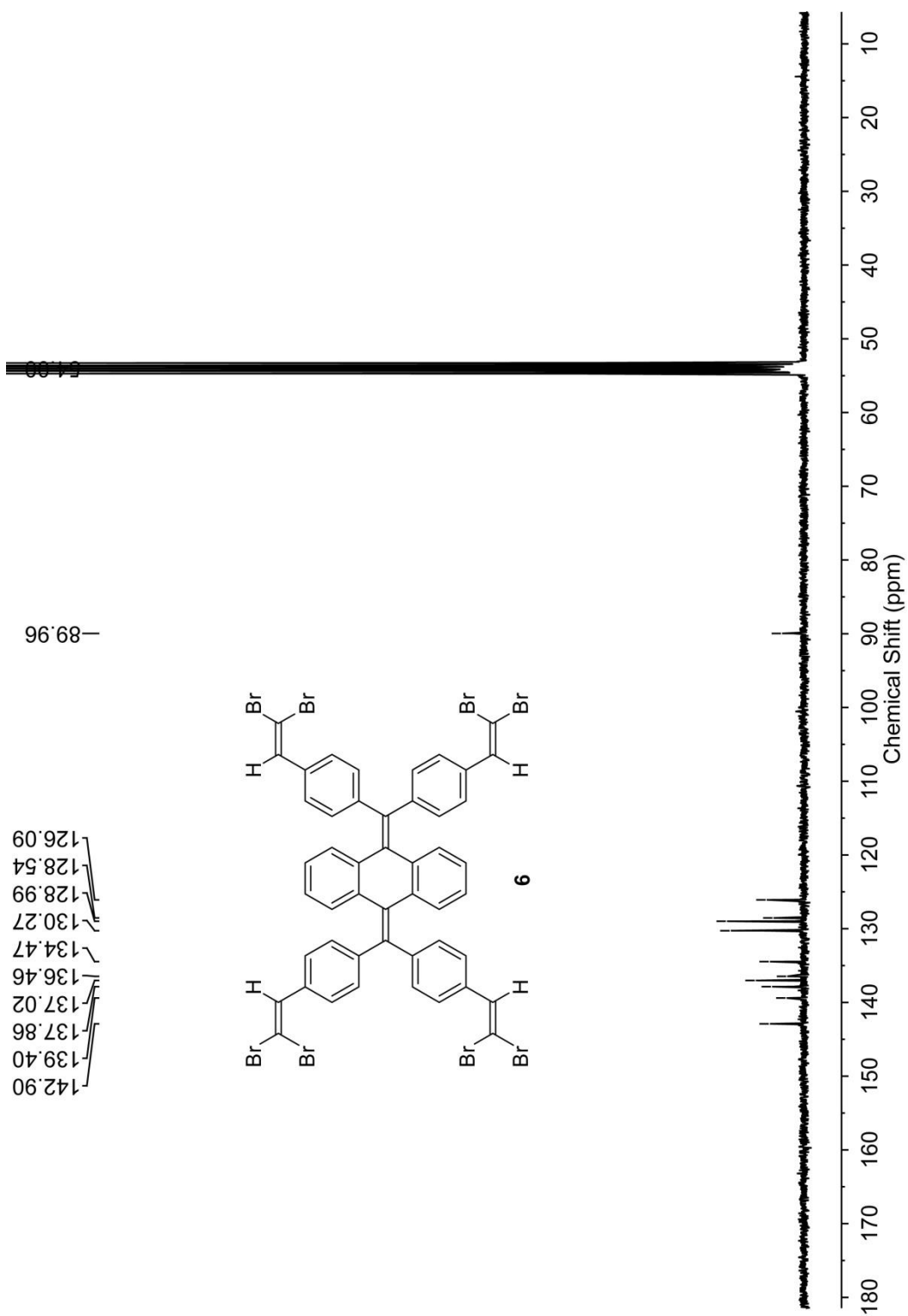


Fig. S-6 ^{13}C NMR (75 MHz, CD_2Cl_2) of compound **6**.

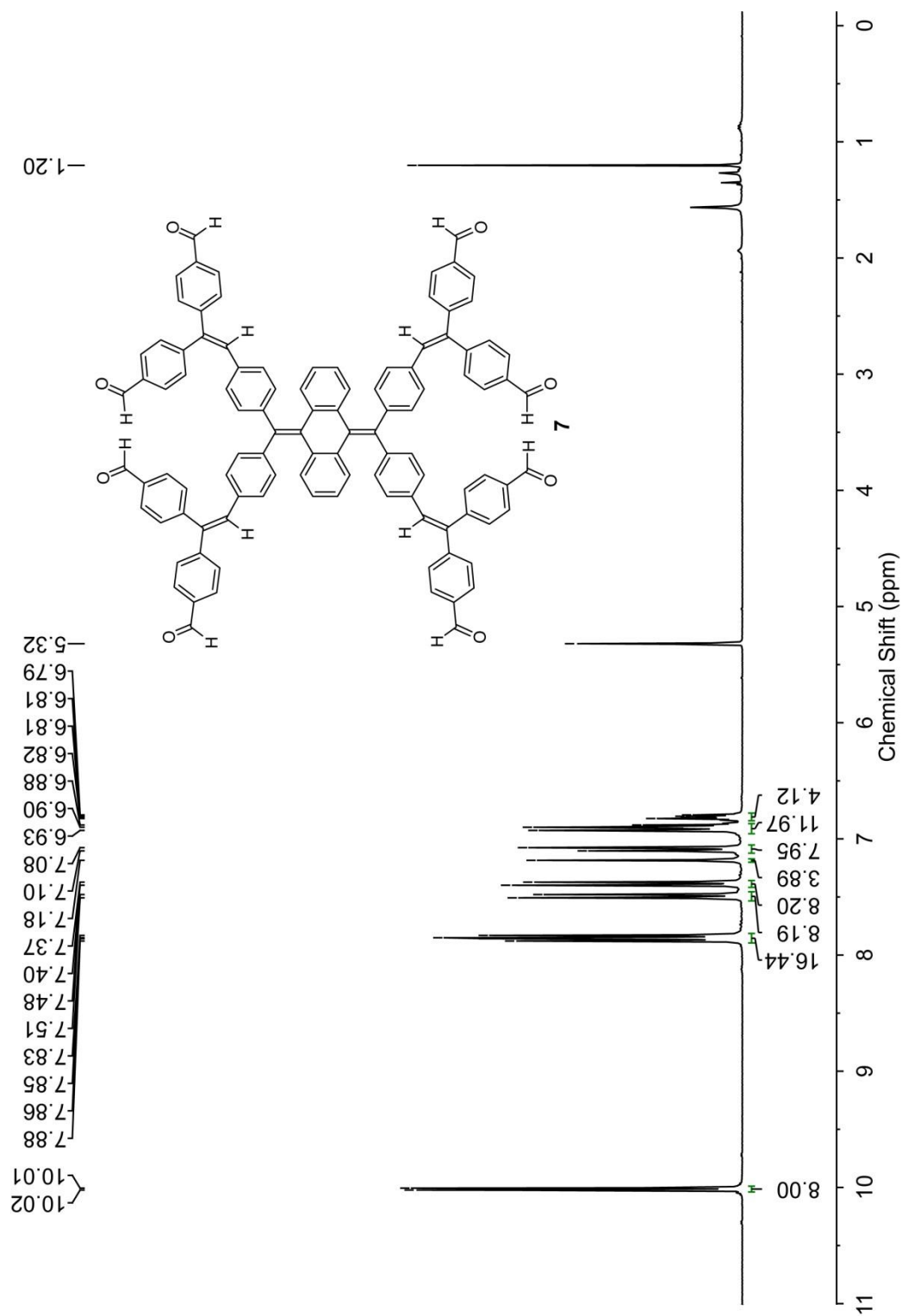


Fig. S-7 ¹H NMR (300 MHz, CD₂Cl₂) of compound 7.

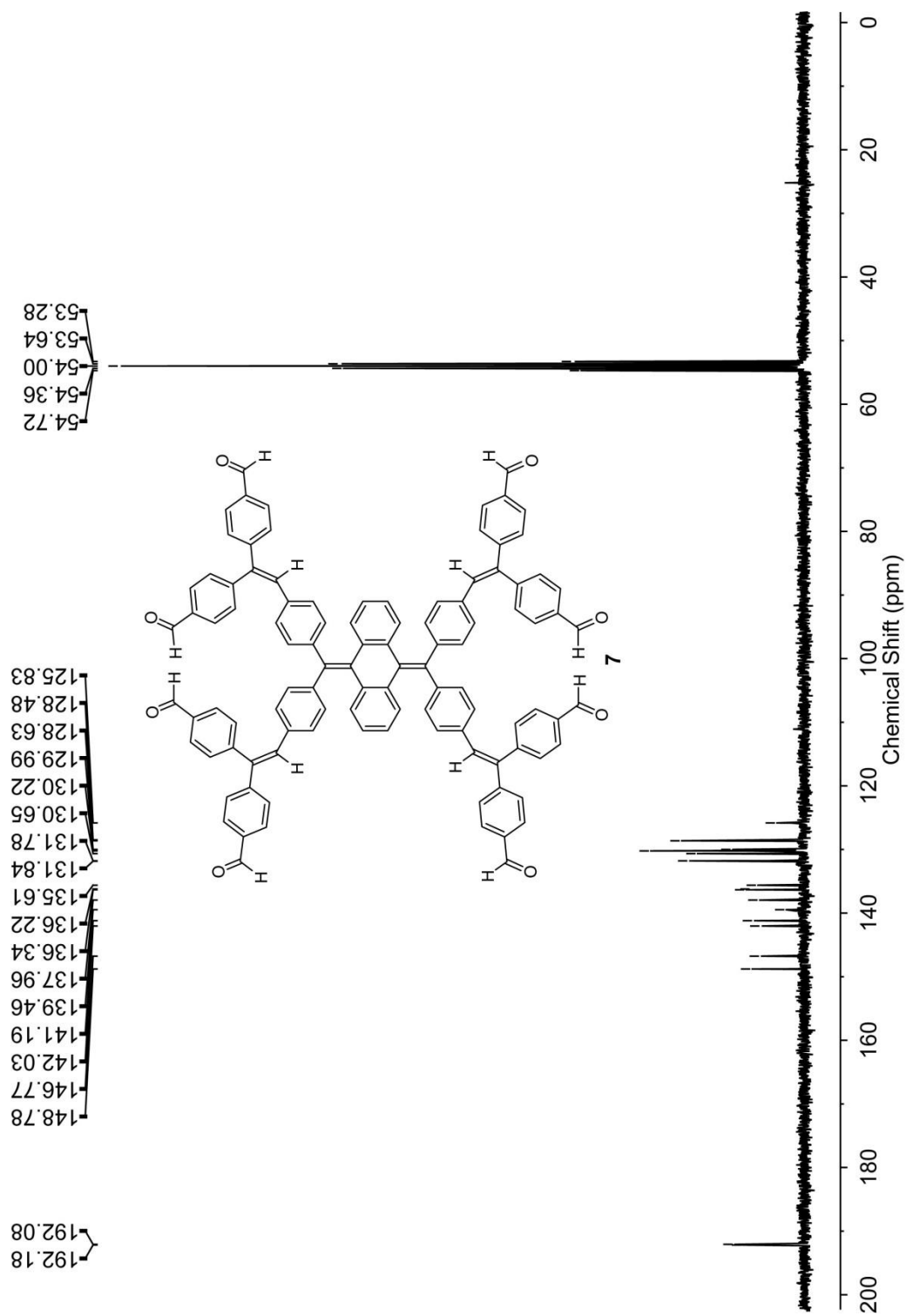


Fig. S-8 ^{13}C NMR (75 MHz, CD_2Cl_2) of compound 7.

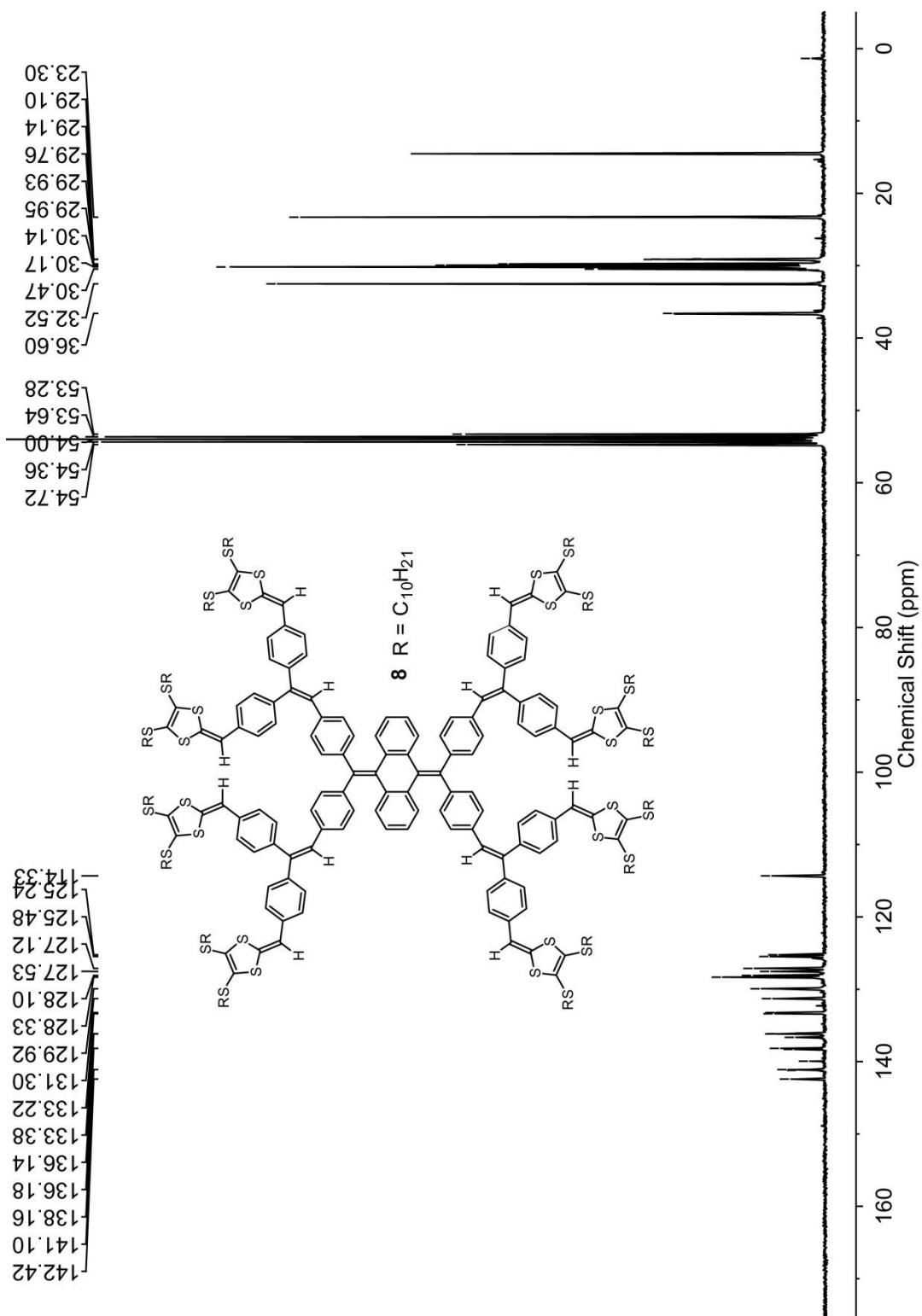


Fig. S-10 ^{13}C NMR (75 MHz, CD_2Cl_2) of compound **8**.

3. UV-Vis Titration Studies

3.1 UV-Vis titration data

Tetrakis(DTF)-AQ **5** and Octa(DTF)-AQ **8** were subjected to UV-Vis titrations with nitrobenzene and three nitrobenzene derivatives (i.e., DNT, TNT, and picric acid) in CHCl_3 respectively. The detailed results are summarized in Fig. S-11 and Fig. S-12.

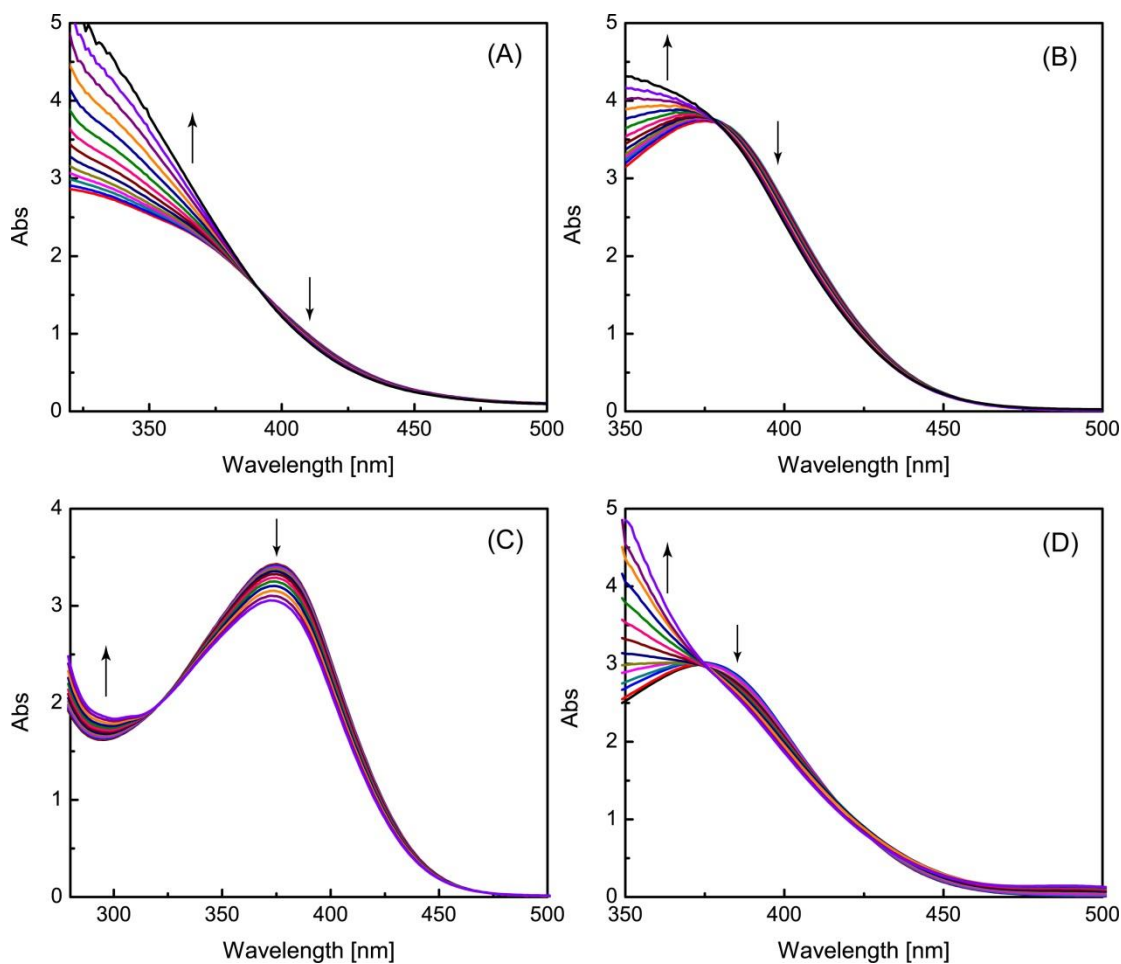


Fig. S-11 UV-Vis titration profiles of compound **5** ($42.7 \mu\text{M}$ in CHCl_3 , 298 K) with (A) nitrobenzene (0 to 3.18 molar equiv), (B) 2,4-dinitrotoluene (0 to 2.15 molar equiv), (C) 2,4,6-trinitrotoluene (0 to 0.34 molar equiv), (D) picric acid (0 to 0.34 molar equiv).

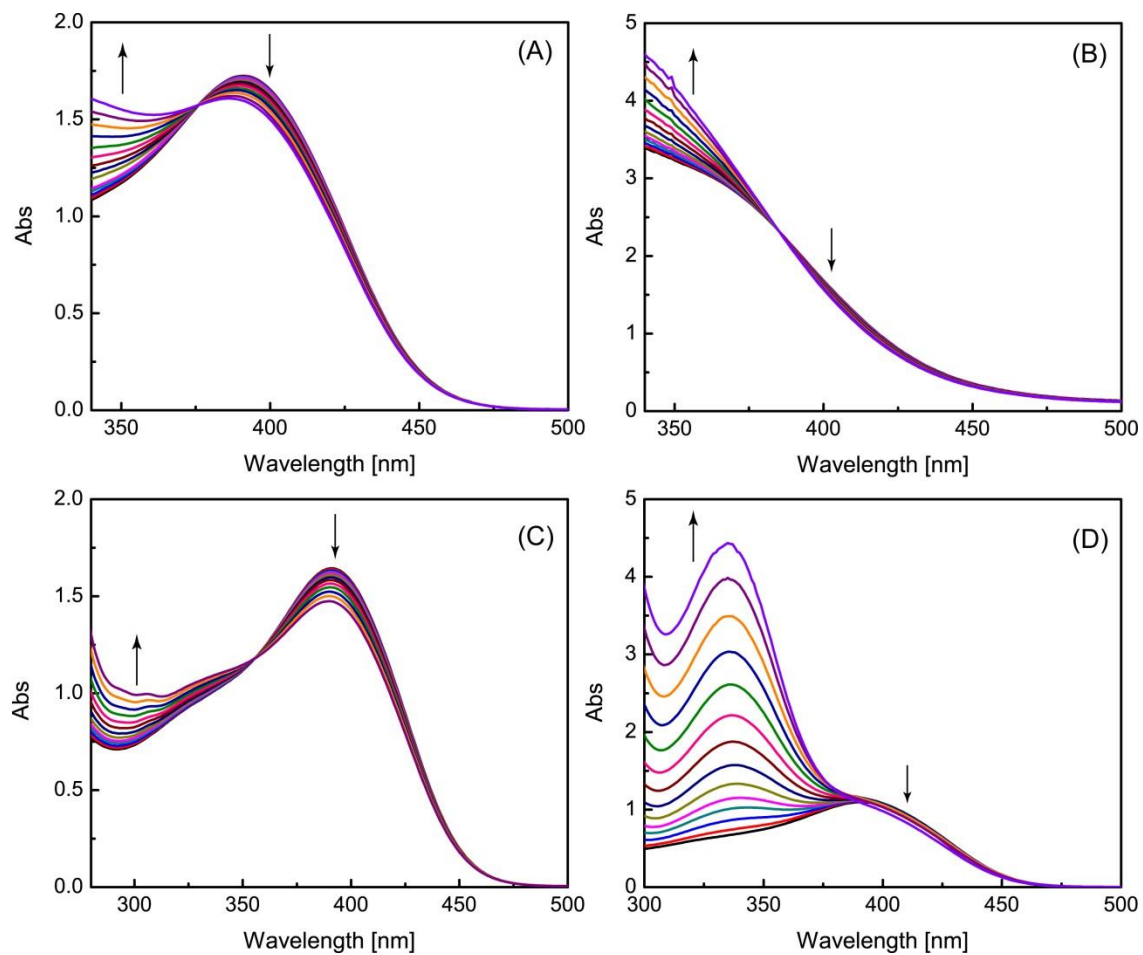


Fig. S-12 UV-Vis titration profiles of compound **8** (20.4 μM in CHCl_3 , 298 K) with (A) nitrobenzene (0 to 6.63 molar equiv), (B) 2,4-dinitrotoluene (0 to 4.48 molar equiv), (C) 2,4,6-trinitrotoluene (0 to 0.72 molar equiv), (D) picric acid (0 to 0.71 molar equiv).

3.2 Job plot analysis

Herein the binding stoichiometry of poly(DTF)-AQs with nitrobenzene derivatives was briefly studied by the analyzing the Job's plot of oct-DTF **8** with nitrobenzene (NB) as a representative case, since not all the UV-Vis titration data in Fig. S11 and Fig. S-12 show clear and significant spectral changes for detailed binding mode analysis. As shown in Fig. S-13, the Job's plot was made by correlating $A - \epsilon[\mathbf{8}]_0$ with the molar fraction of NB, where A is the observed absorbance at 390 nm, ϵ is the extinction coefficient of **8**, and $[\mathbf{8}]_0$ is the initial concentration of **8**.

Assuming that **8** and NB form a 1:1 complex (C) as shown in Eq. S-1,



The observed absorbance at 390 nm can be expressed by Eq. S-2, where ϵ' and ϵ'' stand for the extinction coefficient of the complex (C) and NB respectively.

$$A = \epsilon[\mathbf{8}] + \epsilon'[\text{C}] + \epsilon''[\text{NB}] \quad (\text{Eq. S-2})$$

Considering that $\epsilon'' \approx 0$ at 390 nm and the actual concentration $[\mathbf{8}] = [\mathbf{8}]_0 - [\text{C}]$, the actual concentration of complex [C] can be thus expressed by Eq. S-3, where the term, $A - \epsilon[\mathbf{8}]_0$, can be found to be directly proportional to [C].

$$[\text{C}] = (A - \epsilon[\mathbf{8}]_0)/(\epsilon' - \epsilon) \quad (\text{Eq. S-3})$$

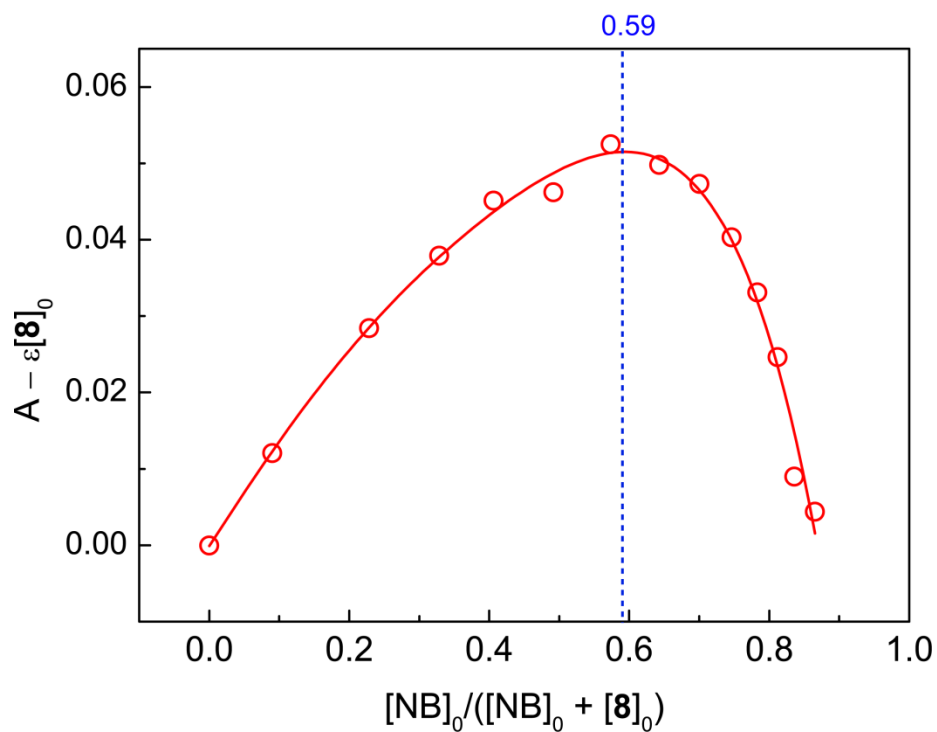


Fig. S-13 Job's plot for determination of the binding stoichiometry of octa(DTF)-AQ **8** with nitrobenzene (NB).

The Job's plot in Fig. S-13 is fit with a polynomial function (5th order) and the maximum appears at the molar fraction = 0.59, which is slightly deviated from the ideal value of 0.5 for the 1:1 binding ratio. This result suggests that 1:1 is the dominant binding ratio, while 1:2 binding may also occur to some extent.

4. Molecular Modeling Studies

The ground-state structures of tetrakis(DTF)-AQ **5**, octa(DTF) **8**, and the 1:1 complex of **5** and nitrobenzene (NB@**5**) were optimized by the semi-empirical PM6 method implemented in Gaussian 09 software package. The frontier molecular orbital (FMO) plots and eigenvalues of **5** and NB@**5** were computed by single-point density functional theory (DFT) calculations at the B3LYP/6-31G(d) level of theory. For all of the calculations, the SC₁₀H₂₁ side chains in the compounds were replaced with hydrogen atoms to save computational expenses.

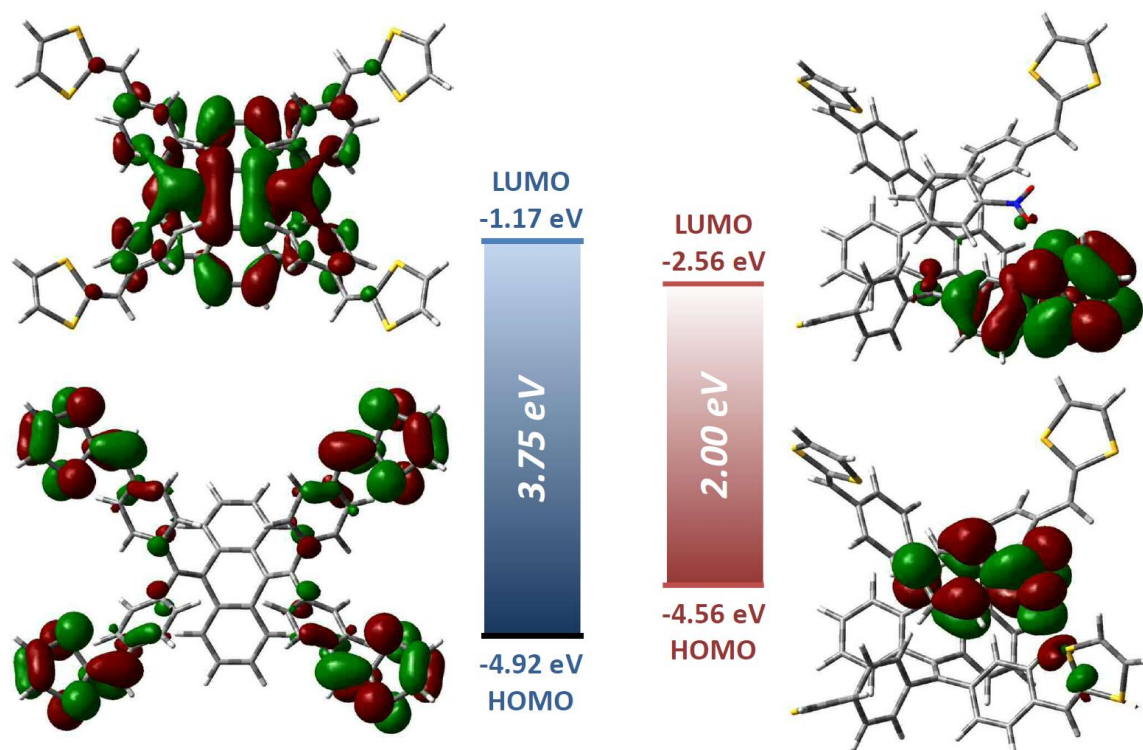


Fig. S-14 Optimized structures and FMOs of compound **5** (left) and the 1:1 supramolecular complex of NB@**5** (right). Structures optimized at the PM6 level and single-point calculations done at the B3LYP/6-31G(d) level of theory. FMO countours are plotted at an isovalue of 0.02.

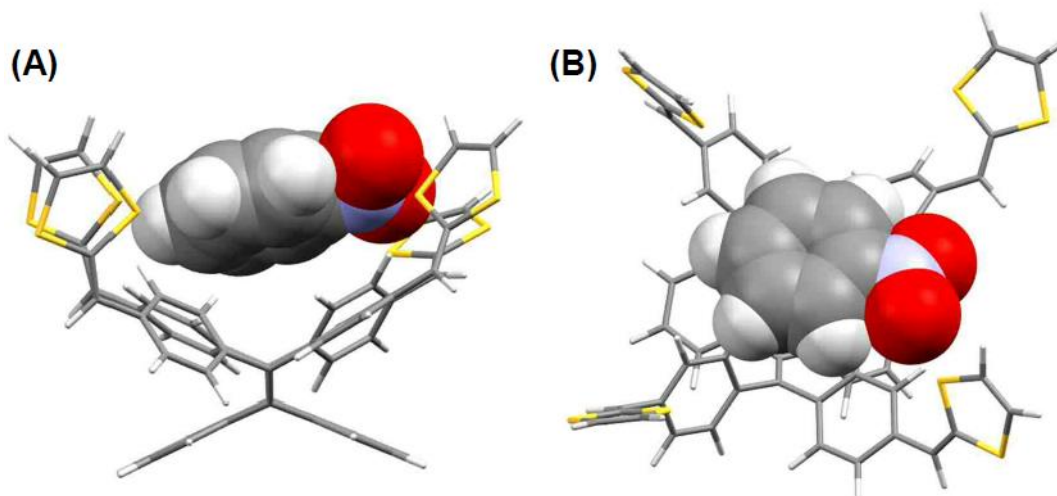


Fig. S-15 Molecular structure of the 1:1 complex of **5** and nitrobenzene (NB@**5**) optimized at the PM6 level. (A) Side view, (B) top view. The NB molecule is highlighted by the space-filling plot to better visualize the intermolecular interactions.

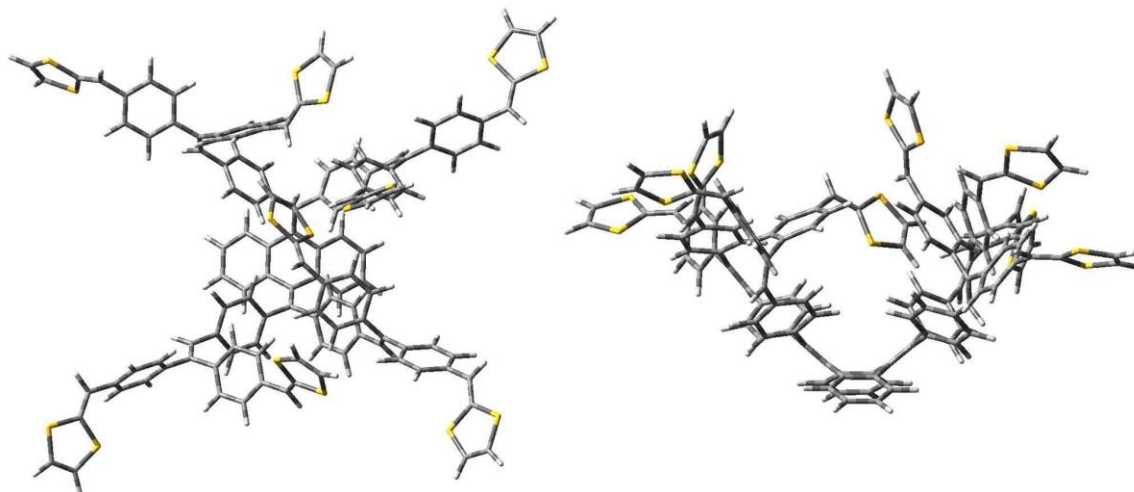


Fig. S-16 Molecular structure of compound **8** optimized at the PM6 level. (A) Top view, (B) side view.

5. SEM Imaging of Poly-[5]

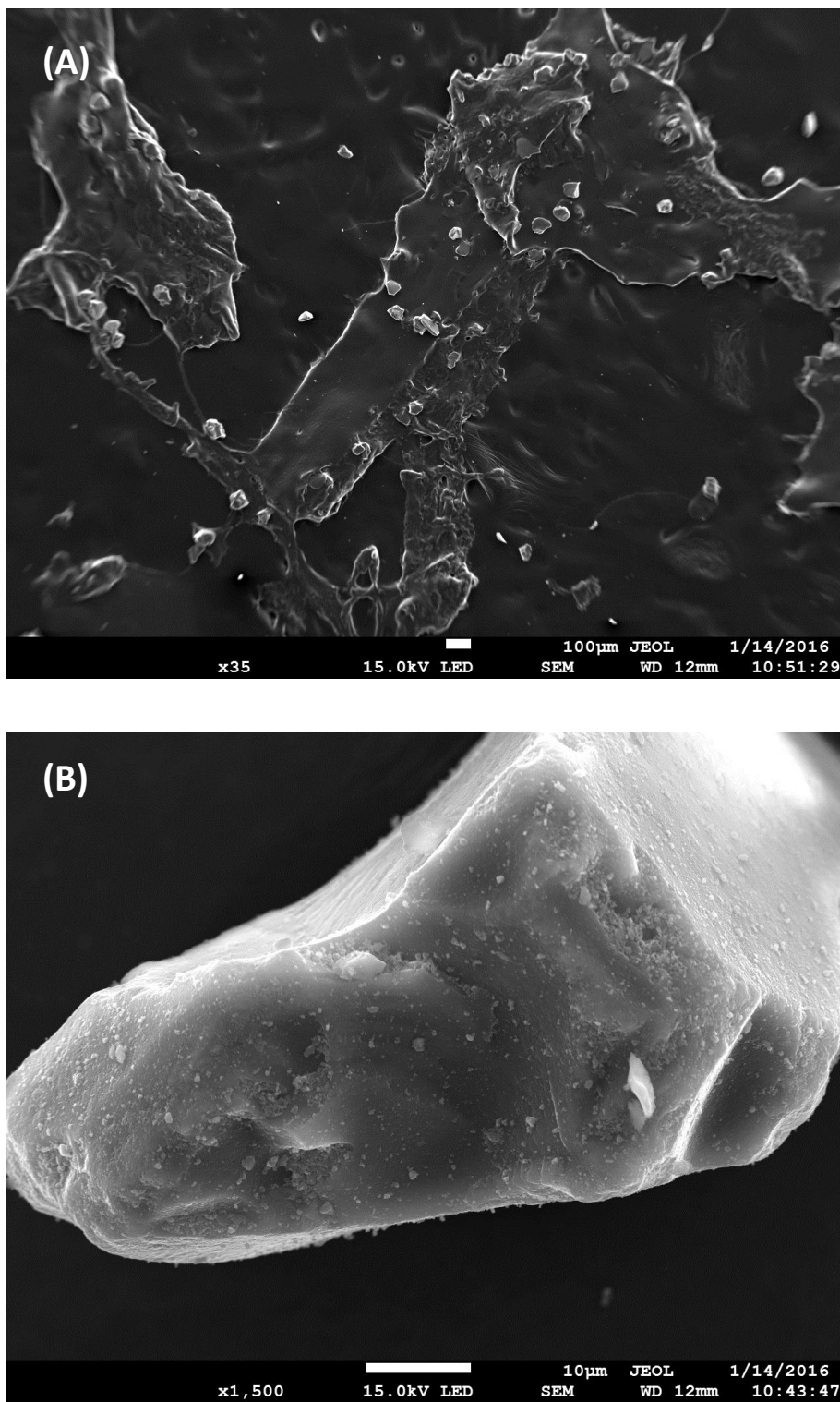


Fig. S-17 SEM images of poly-[5] generated by oxidative coupling reactions.